

Magnetic resonance scanning and image segmentation procedure at 3 T for volumetry of human hippocampal subfields

Bryony Wood^a, Michael J. Knight^a, Demitra Tsivos^{b,c}, Ruth Oliver^a, Elizabeth Coulthard^{b,c} and Risto A. Kauppinen^{a,d,*}

^a *School of Experimental Psychology, University of Bristol, Bristol, UK*

^b *Institute of Clinical Neuroscience, University of Bristol, Bristol, UK*

^c *North Bristol NHS Trust, Bristol, UK*

^d *Clinical Research and Imaging Centre, University of Bristol, Bristol, UK*

Abstract.

BACKGROUND: Recent evidence suggests that dementia affects hippocampal substructures differentially and thus identifying anatomical details of this structure is potentially clinically important. Visualising details of human hippocampal substructures *in vivo* is challenging by imaging due to the small size of the medial temporal lobe structure.

METHODS: MRI data were acquired with a 3 T MR scanner using a 2D multi-echo spin echo pulse sequence at such a spatial resolution to reveal hippocampal subfield boundaries. These images were used to develop a manual segmentation procedure for the hippocampal subfields based on image contrast within the structures and/or geometric constraints by anatomical landmarks.

RESULTS: The T2-images were used to devise a segmentation protocol for Cornu Ammonis (CA) CA1, CA2, CA3, dentate gyrus, subiculum and lumped Stratum Lacunosum + Stratum Moleculare + Stratum Radiatum. The segmentation protocol was applied to MRI data from healthy young and aged controls as well as a small cohort of mild cognitive impairment (MCI) subjects. The reported subfield volumes showed high levels of inter-rater reliability arguing for potential as a tool in documenting subfield volumetry in clinical research.

CONCLUSIONS: A comprehensive and robust MRI protocol which allows the labelling of six separate hippocampal subfields from images acquired with a 3 T clinical scanner is presented to promote hippocampal subfield volumetry of clinical cohorts.

Keywords: Magnetic resonance imaging, hippocampus, subfields, volumetry

1. Introduction

The total hippocampal volume, as quantified from T1-weighted MR images acquired with scanners operating at 1.5 or 3 T [1,3], is valuable in clinical assessment of dementias, including Alzheimer's disease (AD) [10]. The accelerated rate at which the total volume declines has been adopted as a diagnostic imaging biomarker for AD and also used in treatment monitoring [10]. Recent studies indicate that AD may affect substructures of the hippocampus unevenly [4,18]; hence it could be clinically helpful to reveal internal details of hippocampus. Visualisation of hippocampal substructures by MRI is challenging

*Corresponding author: Risto A. Kauppinen, Professor, School of Experimental Psychology, University of Bristol, 12a Priory Road, Bristol, BS8 1TU, UK. Tel.: +44 117 928 8461; E-mail: psrak@bristol.ac.uk.

due to their small volumes, however. Early studies that have quantified hippocampal subfields directly in humans have either used data acquired with ultra-high field MR systems operating at 4 T [17,18,27], 4.7 T [15] or 7 T [23] or scanned post-mortem preparations to achieve spatial resolutions and image contrast sufficient to identify subfield boundaries.

Recent studies demonstrated subfield visualisation from T1 and proton density [12] and T2 MR images [7,26] acquired at a clinical field strength of 3 T. The study by Winterburn and co-workers [22] used 3D T2-weighted data sets to segment five subfields with the required scan times greater than 45 minutes. While such approaches may be used for research, they are inappropriate for use in clinical cohorts. An alternative approach to those above employs hippocampal surface morphometry from standard spatial resolution T1-weighted images to indirectly evaluate volumes of subfields, most notably those of the CA1 region and subiculum [4]. The study of Devanand and co-workers using the surface morphometry approach indicated that conversion from MCI to AD may be associated with greater decline in CA1 and subiculum volumes compared to stable MCI patients.

Identification of the hippocampal subfields in MR images relied initially on neuroanatomical print-atlases [6,14], yet more recently MR-based atlases have been created to represent the average hippocampal anatomy of a given population [8,9,27], typically utilising group-wise registrations [2]. Inter-subject reliability evident in individuals has led to the development of several manual [13,15,17,18,22,23] and automatic [21,27] procedures to aid in the identification of subfield boundaries within the hippocampus. Previous attempts to label subfields scans have typically segmented a small section of the hippocampal body [18,21], with the exception of Winterburn et al. [22], Wisse et al. [23] and Yushkevich et al. [26] who labelled subfields across the entire structure. The previous studies used images either acquired utilising 7 T MR scanner [23] or from prohibitively long scan sessions at 3 T [22].

The aim of this study was to develop a robust MRI data acquisition protocol for 3 T with tolerable acquisition time for clinical cohorts. To achieve this we used a 2D multi-echo spin echo T2 pulse sequence and acquired images with appropriate signal-to-noise-ratio (SNR) and spatial resolution to allow the delineation and/or identification of hippocampal subfield boundaries. Furthermore, our goal was to develop a segmentation protocol for subfields based on contrast differences in the image, boundaries defined in neuroanatomical atlases [6,14] and, where necessary, geometric constraints [13,15,17,21–23,27]. The protocol was initially applied both to neurologically healthy subjects and a small number of MCI participants.

2. Materials and methods

2.1. Subjects

The study used MRI data from 9 participants aged 21–81 years: 2 healthy young subjects, 1 male and 1 female (mean age 21); 3 healthy aged subjects, 2 females and 1 male (mean age 71) and 4 subjects, 3 females and 1 male, with a recent diagnosis of MCI (mean age 76). The diagnosis of MCI was based on Petersen criteria, with patients showing abnormal memory function for their age and level of education [20]. Time between diagnosis and MRI scans was less than 9 months. Ethical approval for the healthy subjects was obtained from the University of Bristol Faculty of Science Research Ethics Committee and approval for all other subjects from the Research Ethics Committee of the North Bristol NHS Trust. All subjects provided written, informed consent for data sharing and acquisition.

2.2. Image acquisition

MR images were acquired on a 3 T Siemens Magnetom Skyra scanner using a 32-channel head coil. T1-weighted images were acquired using a 3D MPRAGE sequence with the following parameters: TR = 2200 ms, TI = 900 ms, alpha flip angle = 9 degrees, FOV = $220 \times 184 \times 230$ mm, resolution = $0.34 \times 0.34 \times 0.80$ mm³ following a 2-fold interpolation in *k*-space. The MPRAGE was repeated twice at 5 minutes acquisition per experiment and the resulting data sets were then registered and averaged. T2-images were acquired using a 2D multi-echo spin echo sequence, based on a vendor-supplied pulse sequence adapted to phase cycle the refocusing pulse, in a scan time of ~12 minutes with the following parameters: TR = 5500 ms, echo spacing = 12 ms, 12 echoes, slice thickness = 1.72 mm, FOV = $184 \times 218 \times 58$ mm³, in-plane resolution = 0.34×0.34 after 2-fold interpolation. The (magnitude) images corresponding to an entire echo train were summed. All T2 MR images were acquired in an oblique plane in which the long axis of the hippocampus was perpendicular to the coronal plane in the resulting images. All image acquisition occurred within one session with a total scan time of ~22 minutes.

2.3. Contrast differences and geometric rules for the identification of subfield boundaries

The T2-weighted images were selected for segmentation of hippocampi, since these images displayed excellent contrast between hippocampal grey matter (GM) and surrounding white matter (WM) of the alveus and fimbria, allowing identification of external hippocampal boundaries. Furthermore, contrast between hippocampal subfields has been found to be pronounced in T2-weighted images [22]. The hippocampi and their subfields were segmented manually using the masking tools on FSL MRI analysis software [11]. Each hippocampus took approximately 2 hours to segment by an expert rater, thus 4 hours per participant.

Subfields were labelled throughout the entirety of the hippocampal structure. The identification of subfields was based on contrast differences, however, in instances, for example for the distinction of the CA subsections, geometric rules given by neuroanatomical atlases [6,14] and previous publications were applied [7,13,15,22–24]. This may compromise anatomical accuracy, overestimating the volume occupied by some subfields and conversely underestimating others, however, when contrast difference cannot be used, geometric rules provide a reliable, reproducible technique.

2.3.1. Identification of subfields in the most anterior hippocampus

The anterior hippocampus emerged as an oval structure discernible from the hypointense WM, however, the subfields within the first few slices could not be reliably distinguished on contrast differences. Therefore, a horizontal line between the lateral and medial extremity of the structure was drawn [15,22,23], the superior portion labelled as CA1 and inferior one as subiculum which is a reliable way of approximating cytoarchitectonic boundaries at lower resolution scans.

The lumped Stratum Lacunosum (SL) + Stratum Radiatum (SR) + Stratum Moleculare (SM) (SL/SR/SM) subfield [22] emerged 2–4 mm posterior to the first anterior slice of the hippocampus (Fig. 1(a)). This was discernible as a hypointense strip within the GM. SL/SR/SM formed a low intensity line across the lateral–medial extremity, with the CA1 occupying superior and subiculum the inferior GM (Fig. 1(a)). More posteriorly, the hyperintense dentate gyrus (DG) emerged in the centre of the SL/SR/SM, as confirmed by neuroanatomical evidence [6,14].

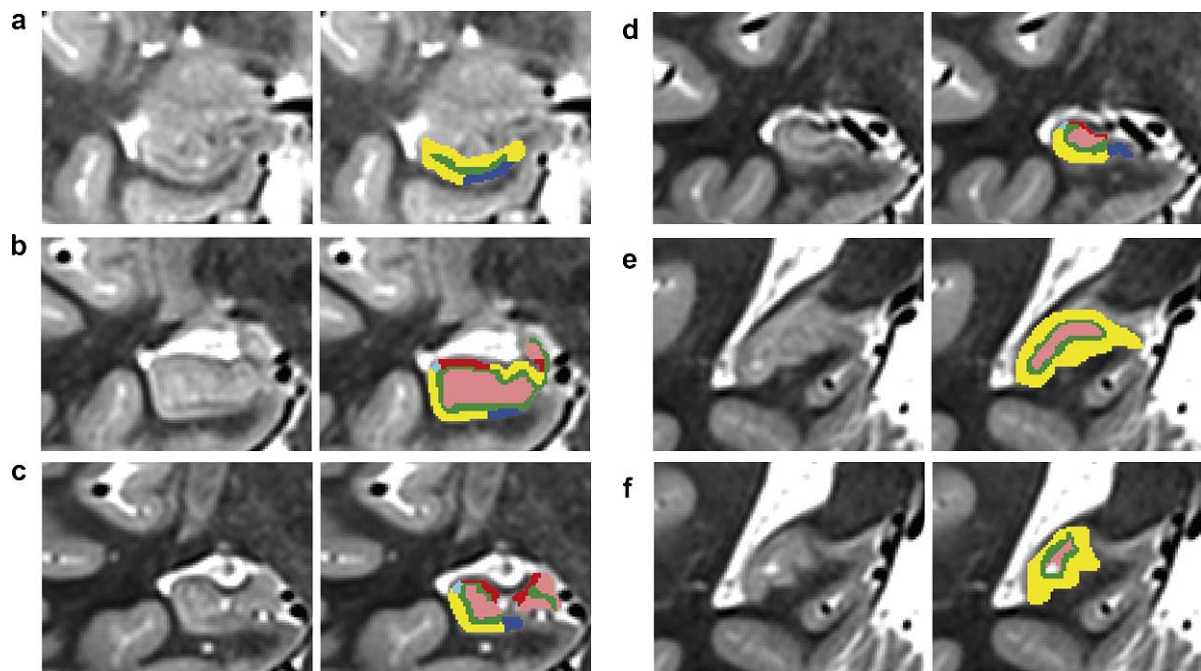


Fig. 1. Hippocampal subfield labelling demonstrated at various points along the anterior–posterior axis of the hippocampus. All slices are taken from a healthy, aged participant. Subfields are highlighted in colours in the images of the right-hand column with the same slice given in the left-hand column. Subfields are represented by the following colours: yellow = CA1, light blue = CA2, red = CA3, dark blue = subiculum, green = SL/SR/SM, pink = DG. (a) An extreme anterior hippocampal slice, whereby only the CA1, SL/SR/SM and subiculum subfields have emerged. (b) A more posterior hippocampal head slice with all six subfields present. (c) The slice where the hippocampus divides into 2 separate portions. (d) A typical hippocampal body slice. (e) The first hippocampal tail slice, whereby the CA2, CA3 and subiculum subfields have disappeared. (f) An extreme posterior hippocampal tail slice. (The colors are visible in the online version of the article; <http://dx.doi.org/10.3233/BSI-150109>.)

2.3.2. Identification of subfields within the hippocampal head

The hippocampal structure extends supero-medially increasing in size, as the head section begins (Fig. 1(b)). Contrast difference was used for SL/SR/SM labelling, the subfield tended to map the shape of the larger, lateral section of the hippocampal head before forming the most medial edge of the supero-medial portion [22]. The DG was contained within the borders of the SL/SR/SM owing to contrast difference (Fig. 1(b)). Upon the emergence of the DG the lateral border of the subiculum was considered to be in-line with the midpoint of the lateral section of the hippocampal head [15]. Thus, the subiculum is located inferior to the SL/SR/SM (Fig. 1(b)). This boundary potentially leads to the underestimation of the subiculum, however, it gives a reliable and reproducible way to separate it from CA, which cannot be done based on contrast difference.

The appearance of the DG was used to indicate the emergence of the CA2 and CA3 based on neuroanatomical [6] and MRI evidence [15,22]. The subfields of the CA were indistinguishable by contrast difference, therefore geometric rules which approximate cytoarchitectonic boundaries were applied according to neuroanatomical [6,14] and previous MRI evidence [22,23]. The CA1 subfield is contained within the infero-lateral portion of the CA, bordered medially by the subiculum and supero-laterally by the CA2. The border between the CA1 and CA2 was considered to be a line extending at 45 degrees from the supero-lateral corner of the SL/SR/SM until the outer edge of the hippocampal GM [6]. The CA2 subfield was considered to occupy a square of the CA, the width of which was determined by the

medial–lateral width of the CA1 [6,14,17,18,22]. This procedure may lead to the underestimation of the CA1 and overestimation of CA3, however, it was adopted as a reproducible technique for CA2 labelling in close approximation to cytoarchitectonic evidence. Furthermore, the contrast of supero-lateral SL/SR/SM as a marker of CA2 provides confidence in approximating cytoarchitectonic boundaries and therefore is more anatomically accurate. The CA3 subfield was considered to be the GM portion between the medial edge of the CA2 and the midpoint of hippocampal head structure (in-line with the lateral border of the subiculum), as suggested in [22]. The remaining GM, extending from the midpoint of the hippocampal head to the most medial border, superior to the SL/SR/SM, but inferior to the most superior outer hippocampal border, forms CA1 [6,14,22]. Figure 1(b) depicts locations of subfields within the hippocampal head.

The SL/SR/SM provides contrast to other subfields in supero-medial portion of the hippocampal head. A geometric rule was applied to divide supero-medial GM into two equally sized portions by a horizontal line running from the lateral extent of the GM to the SL/SR/SM. The superior half was considered to be DG and the inferior portion CA3 (Fig. 1(b)) [22].

2.3.3. Identification of subfields within the hippocampal body

Posterior to the head the hippocampus is divided into two portions (Fig. 1(c)). First, the lateral portion which contains all six subfields. The SL/SR/SM was detectable on contrast to GM forming a C-shaped curvature engulfing the DG (Fig. 1(c)). The subiculum was considered to begin at the most medial point of the DG (Fig. 1(c)) [18,22] based on contrast between the DG and the SL/SR/SM in a close approximation to cytoarchitectonic boundaries [6]. However, this boundary does mean that a small proportion of the prosubiculum is included in the CA1 region, overestimating the overall CA1 volume [18]. The lateral, inferior and superior boundaries of the subiculum could be identified on contrast between hippocampal GM and the surrounding WM of the alveus and fimbria. Similar to the labelling of the CA subfields, the CA1 subfield within this portion fell between the lateral border of the subiculum and the supero-lateral corner of the SL/SR/SM. The CA2 subfield was labelled using the geometric rules above for the hippocampal head and the CA3 subfield was considered to be the medial GM between the end of the CA2 and the most lateral boundary of CA2 superiorly to the SL/SR/SM (Fig. 1(c)).

Second, the medial portion, which contains the SL/SR/SM, CA3 and DG subfields [6,14]. The SL/SR/SM was discernible by contrast and tended to form a line down the centre, from the superior to inferior extent of this portion (Fig. 1(c)). The remaining subfields could not be distinguished on contrast, hence labelling was guided by the location of the SL/SR/SM. The CA3 subfield fell above the superior tip of the SL/SR/SM and the DG occupied the portions laterally and medially to the SL/SR/SM [22]. More posteriorly the medial portion disappeared, but the labelling of the hippocampal subfield continued for the lateral portion for approximately 10–12 slices (Fig. 1(d)).

2.3.4. Identification of subfields within the hippocampal tail

The hippocampal tail was considered to start posterior to the slice where the crura of the fornix is visible in full length [24]. At this point, the SL/SR/SM tends to form a ring within the hippocampal structure (Fig. 1(e)) [6] and, the CA2, CA3 and subiculum subfields are no longer present [6,14]. The ring formed by the SL/SR/SM was discernible from the surrounding GM, the DG was considered to be contained within this ring (Fig. 1(e)), the remaining GM was labelled as CA1 [6,14]. CA1 continued for two to three slices, decreasing in size (Fig. 1(f)). At the extreme tail of the hippocampus the DG disappeared and the SL/SR/SM formed a line, at which point only the SL/SR/SM and the CA1 were labelled. In the most posterior slices (typically one or two slices) the SL/SR/SM was not present and the entire structure was labelled as CA1 [6] until beginning of surrounding WM.

2.4. Volumetric analysis

Following the segmentation of hippocampi, volumetric analysis was performed by extracting each subfield from the image using masks created using the *fslmaths* tool [11] and subsequently performing volumetric analysis using *fslstats* tool [11]. The total volume of each hippocampus was calculated for each participant by summing the volumes calculated of subfields.

2.5. Assessment of reliability of the segmentation protocol

To evaluate the reliability of the segmentation protocol each hippocampus was re-segmented by a second rater (R.O.) in a blinded manner, trained in recognising the contrast differences used to highlight subfield boundaries in the images. Re-segmentation was performed on both the right and left hemispheres of two subjects from each participant group and included all subfields. Reliability was assessed statistically using Dice's volumetric κ , with the following formula being used to quantify the protocol reliability:

$$\kappa = \frac{2a}{2a + b + c},$$

where $2a$ represents the number of voxels shared by the original and re-segmented masks and $b + c$ represents the sum of voxels unique to each mask.

2.6. Comparison of hippocampal volumes measured from T1-weighted and T2-weighted images

To evaluate whether the slice thickness of T2-weighted images impacted the volumetric analysis a T1-weighted image of the right hippocampus was selected from two subjects of each participant group and the total volume calculated. The outer boundaries were manually masked from the anterior–posterior planes using FSL software [11]. Since contrast between hippocampal GM and surrounding temporal lobe WM was less clear in T1-weighted images, the boundaries suggested by the automated *FSL FIRST* tool [19] were used in instances where outer boundaries were difficult to decipher. The T1-volumes were then compared to those obtained from the T2-weighted images using intraclass correlation coefficient (ICC) analysis.

2.7. Assessment of image quality

To assess image quality the contrast-to-noise ratio (CNR) was determined. Briefly, small GM masks from the CA1 of the hippocampus and small WM masks from the temporal lobe directly underneath the hippocampus proper were obtained from one participant from each group (see Fig. 2(b)). The following formula was then applied:

$$\text{CNR} = \frac{|\mu(\text{GM}) - \mu(\text{WM})|}{\sqrt{\sigma^2(\text{GM}) + \sigma^2(\text{WM})}},$$

where μ and σ^2 represent, respectively, the mean and variance of signal intensities in GM and WM masks. To assess whether signal and variability were accurately modelled in the calculations Aedes, Matlab (MATLAB Statistics Toolbox Release, The MathWorks, Inc., Natick, MA, USA) was used to confirm that signal in the selected regions was normally distributed.

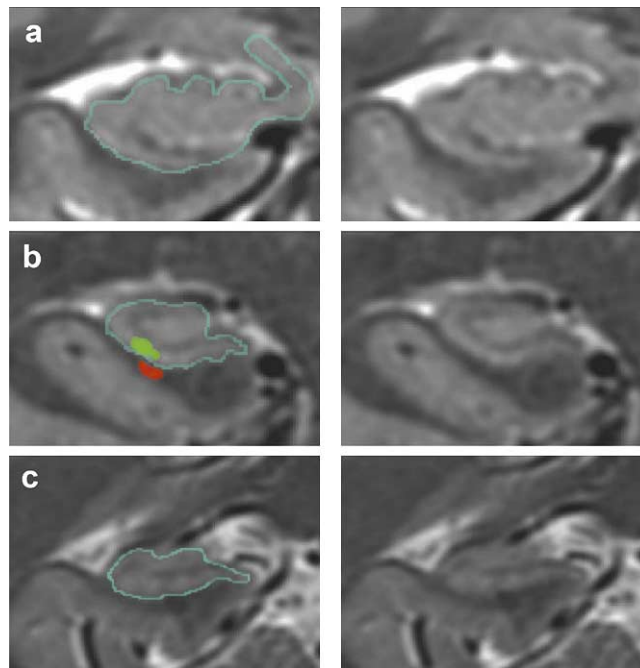


Fig. 2. External HC boundaries demonstrated in the hippocampal head (a), body (b) and tail (c). The masks used for CNR calculation are demonstrated on (b), where green = GM mask and red = WM mask. (The colors are visible in the online version of the article; <http://dx.doi.org/10.3233/BSI-150109>.)

3. Results

3.1. Assessment of image quality

Typical oblique coronal slices through head, body and tail of the hippocampus are shown (Fig. 2). The CNR values for healthy young and aged participants as well as in subjects with MCI were 35.8 (range 25.8–51.5), 27.7 (25.7–28.0) and 21.1 (17.7–24.6), respectively, confirming excellent image quality.

3.2. Contrast differences for the identification of external hippocampal boundaries

In T2-images contrast between hippocampal GM, hypointense WM and hyperintense CSF allowed all outer boundaries of the hippocampal formation to be distinguished (Fig. 2). Throughout the entirety of the formation the most inferior border was identifiable as the point where hippocampal GM met the distinct hypointense WM of the temporal stem. Similarly, the contrast difference evident between the most superior edge of the hippocampal GM and the hypointense WM of the fimbria, bordering the superior edge of the hippocampus proper, could be used to reliably distinguish the upper edge of the hippocampus proper and surrounding WM. Both of these boundaries were clearly distinct on T2 scans. The most lateral border of the hippocampus was identified, again, through the use of contrast between the hypointense band of the fimbria and hippocampal GM, unless, as evident in more posterior slices, this WM structure did not curve round as far as in the most lateral point. When this occurred, the distinction between the hyperintense CSF of the inferior horn of the lateral ventricle and hippocampal GM became the new means of identifying the lateral border of the hippocampus proper. The medial border of the

hippocampus proper was identifiable owing to the contrast between the hyperintense CSF of the ambient cistern and hippocampal GM, with the exception of the initial, most anterior slices. In these sections, the medial hippocampal border was still identifiable due to the contrast to GM and hypointense temporal lobe WM. The posterior hippocampal border, where labelling of the hippocampal structure was terminated, was identified when the GM of the hippocampus became indistinguishable from the surrounding WM. The anterior border was considered to be the slice where the hyperintense uncus apex emerged and labelling began once this structure was identifiable. Contrast differences could be used consistently to identify all outer hippocampal boundaries.

3.3. Contrast differences for the identification of internal subfield boundaries

Subfields were labelled throughout the entirety of the hippocampal structure, from the most anterior to the most posterior boundaries. The lumped SL/SR/SM subfield was identifiable as a hypointense band which could be distinguished from hyperintense subfields. The SL/SR/SM volume tended to map the shape of the outer boundary of the hippocampus and therefore differed in formation, depending on the hippocampal region (Fig. 1(a)–(d)).

The lumped SL/SR/SM subfield could be used to assign surrounding subfields, the CA1 and DG presenting with less conspicuous contrast differences between them, but separated based on geometric rules (see Section 2.3.2). The DG showed a degree of hyperintensity compared to surrounding subfields, although this difference could not always be relied upon. It was noted that hyperintense cysts within this region were common in MCI participants scanned.

Identifying the lumped SL/SR/SM and DG allowed the lateral boundaries of the subiculum to be located within the hippocampal head and body. Subfields are absent from the hippocampal tail (Fig. 1(e), (f)) thus, identification of its anterior and posterior extremities was based on guidelines from literature [6,22]. The medial and inferior boundaries of the subiculum could be deciphered due to the contrast difference to the surrounding WM (Fig. 1(a)–(d)). The superior boundary of subiculum within the hippocampal body was identified by contrast differences (Fig. 1(d)), whereas its other boundaries were drawn using neuroanatomical atlases [6,14]. The CA1, CA2 and CA3 subfield (Fig. 1) segmentation was performed according to geometric rules [18,21–23,27] and guidelines from Duvernoy [6].

3.4. Volumetric analysis

Data for left/right averaged absolute subfield volumes obtained for each participant in the three groups are displayed in Fig. 3. The obtained values for the healthy, young participant group fall within those previously reported [22].

3.5. Dice volumetric κ results

A mean value of 0.7 or greater was obtained for each subfield with the exception of CA2 for which a mean value of 0.51 was obtained (Table 1). It is worth noting that CA2 has lowest absolute volume of all subfields (Fig. 3).

3.6. Assessment of T1 and T2-weighted data

Total hippocampal volumes obtained from T1 and T2 MRI data were compared using a 2-way mixed ICC model which assessed absolute agreement. Single measures ICC gave 0.959, with 95% confidence intervals from 0.729 to 0.994. This high correlation argues for no difference between volumes obtained from T1 and T2 data.

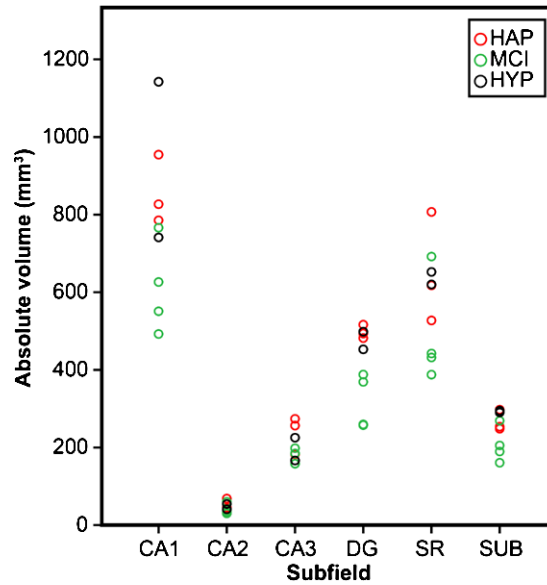


Fig. 3. The left/right averaged subfield volumes (in mm^3) for each participant. HYP – healthy young participants, HAP – healthy aged participants, MCI – mild cognitive impairment participants. (Colors are visible in the online version of the article; <http://dx.doi.org/10.3233/BSI-150109>.)

Table 1
Dice κ results

Subfield	Mean (and range) Dice κ value
CA1	0.76 (0.67–0.98)
CA2	0.51 (0.21–0.69)
CA3	0.7 (0.5–0.89)
Dentate gyrus	0.77 (0.58–0.99)
SL/SR/SM	0.77 (0.64–0.95)
Subiculum	0.78 (0.63–0.98)

Note: Mean κ (range) calculated for each subfield from a sample of two participants in each participant group.

4. Discussion

We describe a robust MRI protocol for 3 T for hippocampal subfield volumetry across the entire length of the formation. The current protocol uses 2D T2-weighted MRI data that are obtained by a multi-echo spin echo pulse sequence providing high image quality for volumetry in a clinically acceptable scan time. The current protocol increases the number of subfields for volumetric analysis to six from recently determined four [7] or five [22,26] from 3 T MR data. The initial experience with the MRI protocol shows that comparable subfield volumes for the CA1, DG, subiculum, SL/SR/SM and combined CA2 + CA3 subfields are obtained from young healthy subjects as previously reported from 3D T2 data [22].

4.1. Data acquisition and image quality

Spatial resolution, SNR and CNR are the critical factors for all structural analysis by MRI, and these factors are strongly interlinked. Previous 3 T MRI protocols have used both 2D [7] and 3D [22] data sets

with rectangular [7] or isotropic [22] voxel dimensions. While in-plane resolution in both approaches are similar, the greater pixel volume benefit SNR in 2D images, which can be used for shorter data collection times, but may compromise anatomical accuracy. Undoubtedly, 3D data set for volumetrics is ideal, however, when T2 images are acquired at 3 T in clinical settings scan time becomes an issue. In hippocampal subfield volumetry the use of an oblique plane in the head-foot direction for 2D acquisition adopted previously [12,26] and used in the current work allowed for comparatively thick slices without loss of essential structural details. This data acquisition strategy maximises SNR (which scales with resolution) and overcomes the need for isotropic resolution adopted in T1-weighted image acquisition in previous work [21,22].

The T2-weighted method of summing over multiple spin echoes used in the study is advantageous for hippocampal subfield volumetry, as the T2 images demonstrate high CNR between GM and WM in line with a recent finding that T2 images display better contrast than afforded by T1-weighted images [22]. This is understandable, as in terms of anatomy, the hippocampus is composed predominantly of GM. The CNR values we report were substantially greater than in recent studies, even after adjusting for both scan time and spatial resolution [22,25]. This factor, which is likely to reflect high SNR in our 2D images, increases the confidence for the current MRI protocol for subfield volumetry. It is anticipated that the current MRI protocol may have wider clinical applications than techniques which rely on ultra-high field scanners [17,18,23]. In this instance it should be noted that the improved SNR afforded by 7 T MRI is offset by the concomitant increase in T1 [5] and decrease in T2 [16] relaxation times in the brain requiring adaptation of data acquisition protocols to obtain suitable contrast for subfield delineation. An interesting observation regarding CNR here was that there is a trend of decreasing with age, the reason for which remains to be studied.

4.2. Segmentation protocol

The manual segmentation protocol using T2 images from 3 T established here allows direct volumetrics of six subfields. Our segmentation protocol exploits T2 contrast to delineate all subfields other than CA1–3, which are labelled according to geometric rules. Where possible we use guidance from previous literature in establishing the segmentation for the entire length of hippocampus, however, as our images were acquired perpendicular to the long axis of hippocampus as supposed to straight coronal plane [22], new segmentation procedures were created. In particular, segmentation of subfields in the head and tail of hippocampus required modifications of the recent protocols [22,23] to avoid inaccuracies in respective subfield volumes. For instance, delineation of boundary between DG and lateral border of subiculum have to be defined differently to the protocol given in [22]. Furthermore, our protocol uses geometric rules to separate CA1, 2 and 3 unlike those previously published [12,13,15]. Although the use of geometric rules potentially compromises anatomical accuracy, they ensure consistency in instances where contrast differences cannot be relied upon. Furthermore, to the best of our knowledge assignment of these subfield boundaries from contrast differences has not been achieved so far, even when ultra-high field scanners are used.

The inter-rater reliability of the segmentation protocol for hippocampal subfields was high as estimated by Dice's volumetric κ . A value greater than 0.7 was calculated for each subfield, with the exception of the small CA2 subfield, suggesting that the protocol is both highly objective and robust. The lower value obtained for CA2 is likely to be because this is the thinnest subfield and the adopted evaluation metric favours structures with a lower surface-area-to-volume ratio. Our values compare favourably with those reported both from long scan time [22] and ultra-high field images [23]. Furthermore, only two previous

papers [22,23] have re-segmented the hippocampal structure along the entirety of the anterior–posterior axis and both of these papers reported comparable intra-rater reliability to the current data.

Despite the widespread use of whole-hippocampus volumetry, there has thus far been very limited literature from subfield volumetry in elderly subjects or AD, which are likely to be important cohorts in the future. Indeed, the study by La Joie et al. [13] is the only one published to date which has applied a comprehensive segmentation on clinical dementia cohorts. However, the segmentation protocol used by La Joie et al. [13] is less comprehensive than ours providing volumes of three separate substructures of hippocampus only.

5. Conclusion

To summarise, we have described an MRI protocol effective at 3 T that within clinically acceptable scan times provides high quality images for hippocampal subfield volumetry. These images were used to devise a comprehensive hippocampal segmentation protocol which allows the identification of six separate subfields along the entire structure, which we believe is suitable for use in both research and clinical work. The protocol shows high level of inter-rater reliability and, when applied to a small cohort of MCI participants and controls reports marked volumetric differences between groups.

Acknowledgements

The study was supported by grants from the Alzheimer Research UK and the BRACE charity. The authors thank Ms. Aileen Wilson for assistance in MRI scanning.

References

- [1] J. Barnes, J.W. Bartlett, L.A. Van De Pol, C.Y. Loy, R.I. Scahill, C. Frost, P. Thompson and N.C. Fox, A meta-analysis of hippocampal atrophy rates in Alzheimer's disease, *Neurobiology of Aging* **30** (2009), 1711–1723.
- [2] M.M. Chakravarty, A.F. Sadikot, J. Germann, P. Hellier, G. Bertrand and D.L. Collins, Comparison of piece-wise linear, linear and nonlinear atlas-to-patient warping techniques: Analysis of the labeling of subcortical nuclei for functional neurosurgical applications, *Human Brain Mapping* **30** (2009), 3574–3595.
- [3] S.G. Csernansky, L. Wang, J. Swank, J.P. Miller, M. Gado, D. Mckeel, M.I. Miller and J.C. Morris, Preclinical detection of Alzheimer's disease: Hippocampal shape and volume predict dementia onset in the elderly, *NeuroImage* **25** (2005), 783–792.
- [4] D.P. Devanand, R. Bansal, J. Liu, X. Hao, G. Pradhaban and B.S. Peterson, MRI hippocampal and entorhinal cortex mapping in predicting conversion to Alzheimer's disease, *NeuroImage* **60** (2012), 1622–1629.
- [5] M.A. Dieringer, M. Deimling, D. Santoro, J. Wuerfel, V.I. Madai, J. Sobesky, F. Von Knobelsdorff-Brenkenhoff, J. Schulz-Menger and T. Niendorf, Rapid parametric mapping of the longitudinal relaxation time T1 using two-dimensional variable flip angle magnetic resonance imaging at 1.5 Tesla, 3 Tesla and 7 Tesla, *PLoS One* **9** (2014), 1–8.
- [6] H.M. Duvernoy, *The Human Hippocampus: Functional Anatomy, Vascularisation and Serial Sections with MRI*, 3rd edn, Springer, New York, 2005.
- [7] M.J. Firbank, A.M. Blamire, A. Teodorczuk, E. Teper, E.J. Burton, D. Mitra and J.T. O'Brien, High resolution imaging of the medial temporal lobe in Alzheimer's disease and dementia with Lewy bodies, *Journal of Alzheimer's Disease* **21** (2010), 1129–1140.
- [8] S. Frey, D.N. Pandya, M.M. Chakravarty, L. Bailey, M. Petrides and D.L. Collins, An MRI based average macaque monkey stereotaxic atlas and space (MNI monkey space), *NeuroImage* **55** (2011), 1435–1442.
- [9] G. Grabner, A.L. Janke, M.M. Budge, D. Smith, J. Pruessner and D.L. Collins, Symmetric atlas and model based segmentation: An application to the hippocampus in older adults, in: *Medical Image Computing and Computer-Assisted Intervention*, Toronto, 2006, R. Larsen, M. Nielsen and J. Sporrang, eds, LNCS, Vol. 4191, Springer, 2006, pp. 58–66.

- [10] C.R. Jack, Alzheimer disease: New concepts on its neurobiology and the clinical role imaging will play, *Radiology* **263** (2012), 344–361.
- [11] M. Jenkinson, C.F. Beckmann, T.E. Behrens, M.W. Woolrich and S.M. Smith, FSL, *NeuroImage* **62** (2012), 782–790.
- [12] R. La Joie, M. Fouquet, F. Mezenge, B. Landeau, N. Villain, K. Mevel, A. Pelerin, F. Eustache, B. Desgranges and G. Chetelat, Differential effect of age on hippocampal subfields assessed using a new high-resolution 3 T MR sequence, *NeuroImage* **53** (2010), 506–514.
- [13] R. La Joie, A. Perratin, V. De La Sayette, S. Egret, L. Dœuvre, S. Belliard, F. Eustache, B. Desgranges and G. Chetelat, Hippocampal subfield volumetry in mild cognitive impairment, Alzheimer’s disease and semantic dementia, *NeuroImage: Clinical* **3** (2013), 155–162.
- [14] J.K. Mai, G. Paxinos and T. Voss, *Atlas of the Human Brain*, 3rd edn, Academic Press, London, 2008.
- [15] N.V. Malykhin, R.M. Lebel, N.J. Coupland, A.H. Wilman and R. Carter, *In vivo* quantification of hippocampal subfields using 4.7 T fast spin echo imaging, *NeuroImage* **49** (2010), 1224–1230.
- [16] F. Mitsumori, H. Watanabe, N. Takaya, M. Garwood, E.J. Auerbach, S. Michaeli and S. Mangia, Toward understanding transverse relaxation in human brain through its field dependence, *Magnetic Resonance in Medicine* **68** (2012), 947–953.
- [17] S. Mueller and M. Weiner, Selective effect of age, Apo e4 and Alzheimer’s disease on hippocampal subfields, *Hippocampus* **19** (2009), 558–564.
- [18] S.G. Mueller, L. Stables, A.T. Du, N. Schuff, D. Truran, N. Cashdollar and M.W. Weiner, Measurement of hippocampal subfields and age-related changes with high-resolution MRI at 4 T, *Neurobiology of Aging* **28** (2007), 719–726.
- [19] B. Patenaude, S.M. Smith, D. Kennedy and M. Jenkinson, A Bayesian model of shape and appearance for the subcortical brain, *NeuroImage* **56** (2011), 907–922.
- [20] R.C. Petersen, G.E. Smith, S.C. Waring, R.J. Ivnik, E. Kokmen and E.G. Tangelos, Aging, memory, and mild cognitive impairment, *International Psychogeriatrics* **9** (1997), 65–69.
- [21] K. Van Leemput, A. Bakkour, T. Benner, G. Wiggins, L.L. Weld, J. Augustinack, B.C. Dickerson, P. Golland and B. Fischl, Automated segmentation of hippocampal subfields from ultra-high resolution *in vivo* magnetic resonance imaging, *Hippocampus* **19** (2009), 549–557.
- [22] J.L. Winterburn, J.C. Pruessner, S. Chavez, M.M. Schira, N.J. Lobaugh, A.N. Varieskos and M.M. Chakravarty, A novel *in vivo* atlas of human hippocampal subfields using high-resolution 3 T magnetic resonance imaging, *NeuroImage* **74** (2013), 254–265.
- [23] L.E.M. Wisse, L. Gerritsen, J.J.M. Zwanenburg, H.J. Kuijf, P.R. Luijten, G.J. Biessels and M.I. Geerlings, Subfields of the hippocampal formation at 7 T magnetic resonance imaging: *In vivo* volumetric assessment, *NeuroImage* **61** (2012), 1043–1049.
- [24] P.A. Yushkevich, R.S.C. Amaral, J.C. Augustinack, A.R. Bender, J.D. Bernstein, M. Boccardi, M. Bocchetta, A.C. Burggren, V.A. Carr, M.M. Chakravarty, G. Chetelat, A.M. Daugherty, L. Davachi, S.L. Ding, A. Ekstrom, M.I. Geerlings, A. Hassan, Y. Huang, J.E. Iglesias, R. La Joie, G.A. Kerchner, K.F. La Rocque, L.A. Libby, N. Malykhin, S.G. Mueller, R.K. Olsen, D.J. Palambo, M.B. Parekh, J.B. Pluta, A.R. Preston, J.C. Pruessner, C. Ranganath, N. Raz, M.L. Schlichting, D. Schoemaker, S. Singh, C.E.L. Stark, N. Suthana, A. Tomparry, M.M. Turawski, K. Van Leemput, A.D. Wagner, L. Wang, J.L. Winterburn, L.E.M. Wisse, M.A. Yassa, M.M. Zeineh and The Hippocampal Subfields Group, Quantitative comparison of 21 protocols of labelling hippocampal subfields and parahippocampal subregions in *in vivo* MRI: Towards a harmonised segmentation protocol, *NeuroImage* (2015), to appear; DOI:10.1016/j.neuroimage.2015.01.004.
- [25] P.A. Yushkevich, B.B. Avants, J. Pluta, S. Das, D. Minkoff, D. Mechanic-Hamilton, S. Glynn, S. Pickup, W. Liu, J.C. Gee, M. Grossman and J.A. Detre, A high-resolution computational atlas of the human hippocampus from postmortem magnetic resonance imaging at 9.4 T, *NeuroImage* **44** (2009), 385–398.
- [26] P.A. Yushkevich, J.B. Pluta, H. Wang, L. Xie, S.L. Ding, E.C. Gertje, L. Mancuso, D. Kilot, S.R. Das and D.A. Wolk, Automated volumetry and regional thickness analysis of hippocampal subfields and medial temporal cortical structures in mild cognitive impairment, *Human Brain Mapping* **36** (2015), 258–287.
- [27] P.A. Yushkevich, H. Wang, J. Pluta, S.R. Das, C. Craige, B.B. Avants, M.W. Weiner and S. Mueller, Nearly automatic segmentation of hippocampal subfields in *in vivo* focal T2-weighted magnetic resonance imaging, *NeuroImage* **53** (2010), 1208–1224.